



● *Original Contribution*

## PARAMETRIC ANALYSIS OF CAROTID PLAQUE USING A CLINICAL ULTRASOUND IMAGING SYSTEM

KENDALL R. WATERS,<sup>\*,1</sup> S. LORI BRIDAL,<sup>\*</sup> CLAUDE COHEN-BACRIE,<sup>†</sup> CLAIRE LEVRIER,<sup>†</sup>  
PAUL FORNÈS<sup>‡</sup> and PASCAL LAUGIER<sup>\*</sup>

<sup>\*</sup>Laboratoire d'Imagerie Paramétrique, UMR 7623 CNRS, Université Paris VI, Paris, France; <sup>†</sup>Philips Research France, Suresnes, France; and <sup>‡</sup>Laboratoire d'Anatomie Pathologique, Hôpital Européen Georges Pompidou, Paris, France

(Received 23 December 2002; revised 25 July 2003; in final form 5 August 2003)

**Abstract**—We evaluated quantitative ultrasonic methods for assessment of carotid plaque content. *In vitro* measurements of fixed, carotid plaque specimens obtained by surgical endarterectomy were performed using a clinical Philips HDI 5000 imaging system connected to a radiofrequency (RF) signal-acquisition system. We acquired RF signals and grey-scale images from carotid specimens ( $n = 17$ ) and a tissue-mimicking reference phantom. Imaged plaque sections were then classified according to histology. Parametric images were constructed from the integrated backscatter (IBS), and the midband, slope and intercept values of a straight-line fit to the apparent backscatter transfer function. Analysis was performed on 82 regions-of-interest (ROIs). The IBS values for collagen, lipid and hemorrhage plaques were  $5.8 \pm 5.4$ ,  $3.9 \pm 3.7$ ,  $2.8 \pm 2.2$  dB, respectively. Midband and IBS parameter images exhibited good agreement in morphology with histology, whereas the slope and intercept parameter images were noisy. Mean IBS, midband, and grey-scale values of complex plaques were found to be statistically different ( $p < 0.05$ ) from lipid, hemorrhage and fibrolipid plaques. The bias and limits of agreement ( $1.3 \pm 4.9$  dB) between the grey-scale and IBS methods, however, indicated that the two methods were not interchangeable. Results indicate necessary improvements, such as reduction of large measurement variances and identification of robust parameters, that will permit multiparametric characterization of carotid plaque under *in vivo* conditions. (E-mail: krwaters@boulder.nist.gov) © 2003 World Federation for Ultrasound in Medicine & Biology.

**Key Words:** Atherosclerosis, Tissue characterization, *In vitro* measurement, Carotid plaque, Ultrasonic backscatter, Parametric image, Backscatter transfer function, Integrated backscatter, Mid-band, Slope, Intercept, Grey-scale, Bias, Limits of agreement, Significant correlation.

### INTRODUCTION

Atherosclerosis is a primary cause of heart disease and stroke, which is estimated to be the underlying cause of 50% of deaths in westernized countries (Lusis 2000). Composition and structure of atherosclerotic plaques have been identified as factors influencing the clinical risk (Davies and Thomas 1985; Loree et al. 1992) that is associated with rupture, ulceration and thrombosis, as well as the response of the plaque to interventional or pharmacological therapies (Coy et al. 1992). Consequently, a noninvasive technique permitting the evaluation of plaque composition before treatment could pro-

vide useful information for the evaluation of patient risk and guidance of therapeutic decisions and monitoring.

The carotid artery is a site of atherosclerotic plaque formation that could particularly benefit from the development of such a technique. Currently, the decision for carotid plaque removal is based primarily on the level of stenosis. Of the methods available for revascularization, surgical intervention (*i.e.*, endarterectomy) may be the most appropriate for fragile and highly stenotic plaques (NASCET 1991). In other cases, intraluminal or pharmacological approaches could provide less invasive alternatives.

A large percentage of carotid plaques responsible for stroke are easily accessible to noninvasive ultrasonic evaluation. Although ultrasonic duplex imaging (*i.e.*, Doppler and grey-scale) of the carotid artery is routinely used in the clinic to assess the level of stenosis and blood

<sup>1</sup>Dr. Waters' current address is National Institutes of Standards and Technology, Materials Reliability Division, Boulder, CO 80305 USA.

Address correspondence to: Dr. K. R. Waters, National Institutes of Standards and Technology, Materials Reliability Division, Boulder, CO 80305 USA. E-mail: krwaters@boulder.nist.gov

flow, the evaluation of plaque composition that can be obtained from such images remains limited. Several approaches for the evaluation of atherosclerotic plaque composition using ultrasonic images have been explored. Qualitative methods have been proposed to visually evaluate plaque morphology, brightness and heterogeneity (Gronholdt et al. 1997, 1998). Quantitative approaches involving computer-assisted estimation of image texture (Wilhjelm et al. 1998) or mean grey-scale have also been proposed (Urbani et al. 1993). Although such systematic approaches to image evaluation provide additional information related to plaque content, the assessment of the image can be strongly dependent on system settings, such as image compression techniques, time-gain-compensation (TGC) levels, and beam-focusing parameters.

Quantitative approaches based upon the analysis of radiofrequency (RF) signals aim to remove system-dependent effects on the signal backscattered from the atherosclerotic plaque. Such quantitative tissue characterization is based upon the principle that architectural alterations resulting from disease processes may modify the scattering and propagation of the ultrasound (US) in the tissues (Campbell and Waag 1983; Lizzi et al. 1983). The application of appropriate signal analysis techniques can provide estimates of the US propagation and scattering properties (Barzilai et al. 1987; Picano et al. 1988) and strain-based properties (de Korte et al. 2000) of vascular tissues. These may potentially provide additional objective information of diagnostic significance.

The objective of this investigation was to demonstrate that RF signals (5 to 9 MHz) acquired with a clinical US imaging system using a linear array can potentially be used for the noninvasive, quantitative characterization of carotid arterial plaque under *in vivo* conditions. The feasibility of this approach is demonstrated *via in vitro* measurements of formalin-fixed, human carotid plaque specimens. Quantitative parametric images of carotid plaque specimens are constructed from the analysis of ultrasonic RF measurements. We compare the analysis of grey-scale images of plaque sections with the analysis of the corresponding US RF measurements. Plaque content is determined by histologic evaluation of the plaque specimens. The correspondence between the RF, grey-scale and histologic results is discussed.

## MATERIALS AND METHODS

### *Ultrasonic imaging system*

Ultrasonic measurements were performed using a Philips HDI 5000 US imaging system (Philips, Bothell, WA) with a linear array (L12-5 50; 7.5-MHz) that had a 6-dB down bandwidth of approximately 5 to 9 MHz. The imaging system was connected to a digitizer (24-MHz sampling rate) that permitted acquisition of the RF sig-

nals subsequent to beam formation. The transmit field had a single focal zone set at 2.3 cm. The mechanical index (MI) and thermal index (TI) were set to 0.31 and 0.0, respectively. The TGC levels were maintained uniform throughout a 4.8-cm field-of-view (FOV), but the overall gain level was varied between acquisitions to optimize the available dynamic range. No other system settings were changed between measurements.

### *Carotid plaque specimens*

Carotid plaque specimens were collected from 17 patients (11 men, 6 women) who underwent endarterectomy. The mean age of the patients was 73 years (range: 54 to 91 years). The carotid plaque specimens were surgically removed as casts of the carotid bifurcation being devoid only of the adventitia and most of the media, and were kept circumferentially intact. Each plaque specimen was roughly 1 cm in diameter, with a length that varied from 0.5 to 4 cm. Following removal, specimens were placed in a fixative solution (4% formalin). A discussion of the effects due to fixation of the plaque specimens can be found in the Discussion section.

### *Tissue-mimicking phantom*

A multipurpose tissue-mimicking phantom (Model 550-5, ATS Laboratories, Inc., Bridgeport, CT) served as a reference material (Madsen 1993; Zagzebski et al. 1993). The phantom provided a well-characterized medium with homogeneous scattering properties (velocity = 1450 m/s, slope of attenuation = 0.497 dB/cm/MHz). The use of a tissue-mimicking phantom as a reference medium has been proposed as a means to correct for the diffraction properties of an ultrasonic probe (Fink and Cardoso 1984). In addition, the phantom is potentially a convenient reference material for both *in vitro* and *in vivo* measurements, in particular because the modest amplitude of backscattering from such a phantom permits the use of the same or similar TGC levels as for soft tissues. This is an advantage over techniques using planar reflectors that have relatively large reflection coefficients, for which saturation of the receive electronics becomes a concern.

### *Ultrasonic data acquisition*

A series of ultrasonic measurements were performed for each carotid plaque specimen. The plaque specimen was immersed in a room-temperature water bath. The specimen was positioned near the nominal focal zone of the linear array, so that the surface of the plaque was approximately 20 mm from the face of the probe. See Fig. 1 for a diagram of the experimental setup. A cursory scan of each specimen was initially performed with the linear array oriented so that circular cross-sections of the plaque were imaged while translating the

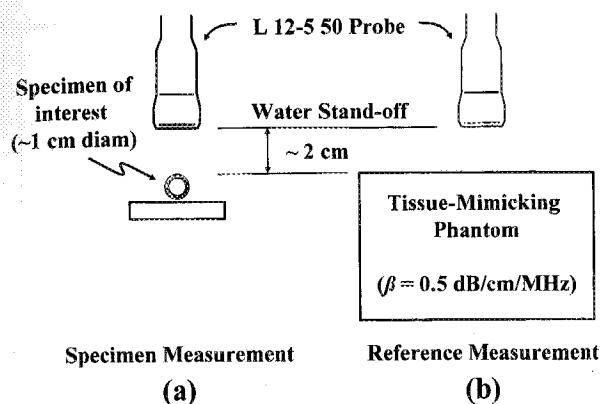


Fig. 1. (a) Diagram representing the experimental setup for data acquisitions performed for each carotid plaque specimen. Each specimen is immersed in a room-temperature water bath and placed near the focal distance of the ultrasonic probe (near 2.3 cm). (b) A similar reference measurement is performed using a tissue-mimicking phantom.

array along the long axis of the plaque. This permitted the identification of spatially independent, highly stenotic sections of plaque that had a minimal presence of calcification, which is generally associated with high echogenicity. The TGC levels were adjusted so that no saturation of the ultrasonic signal occurred. Ultrasonic measurements were made at 62 spatially independent transverse planes of the 17 plaque specimens. Approximately three to four measurements were made for each specimen, but this varied between one and seven measurements, depending on the length of the plaque specimen. Sets of ultrasonic RF signals and grey-scale images of each plane were then acquired and saved to disk for off-line analysis.

For each acquisition of a carotid specimen, a corresponding measurement was made of the phantom (Fig. 1b) with a water stand-off. The same system settings (*e.g.*, TGC levels) were used, and the distance between the face of the probe and the surface of the phantom was the same as the distance between the face of the probe and the surface of the plaque. Representative grey-scale images of a carotid plaque section and the phantom are shown in Fig. 2.

### Histology

Following the ultrasonic acquisitions for each plaque specimen, the imaged plaque sections were marked to permit orientation of histologic sections with respect to ultrasonic images, and then prepared for histology (Bridal *et al.* 1997b). Sections (3- $\mu$ m thick) were stained with hematoxylin-eosin-saffron (HES) for identification of cells and connective tissue. Histologic sec-

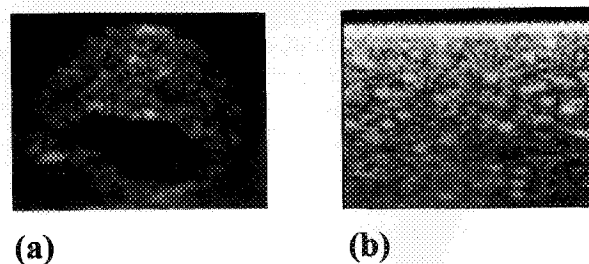


Fig. 2. Representative grey-scale images of (a) a carotid plaque specimen and (b) the tissue-mimicking phantom.

tions were then viewed using an optical magnifier (Wild Heerbrugg M7 S, Leica Microsystems, Wetzlar, Germany) and an optical microscope (Leitz Aristoplan, Leica Microsystems). Digital images (100 $\times$  magnification) of the magnified histologic sections were acquired using a charge coupled device (CCD) 3 camera (KY-F55B, JVC, Yokohama, Japan) and digital image acquisition software (Perfect Image V5.3, Clara Vision, Orsay, France). The selection of the histology regions to image at this magnification was based on the presence of morphologic markers in the images of the plaques and the location of regions selected from ultrasonic parametric images, as discussed in more detail in the Region-of-interest selection section.

A pathologist, who was "blind" to the corresponding ultrasonic images and results, quantitatively classified the plaque content by examination of histologic sections identified in the digitized images of the histologic sections (Bridal *et al.* 1997a). Figure 3a, b, c shows microscopic (100 $\times$  magnification) histology images of representative ROIs of collagen (fibrous), lipid and hemorrhage plaques, respectively. In this study, regions were assigned one of eight plaque classifications: collagen or fibrous (F), lipid (L), intraplaque hemorrhage (H), fibro-lipid (FL), lipid-hemorrhage (LH), fibrocalcification (FCa), fibrohorrhage (FH) and complex (Com) plaques. Complex plaques contained at least three of the

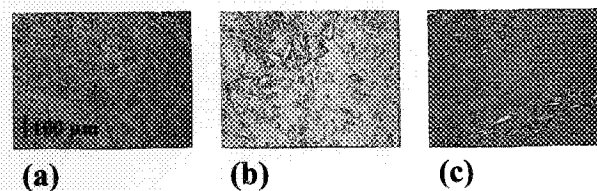


Fig. 3. Microscopic images (100 $\times$  magnification) of histologic ROIs of (a) a collagen plaque, (b) a lipid plaque, and (c) a hemorrhage plaque.

four plaque constituents of collagen, lipid, intraplaque hemorrhage and calcification. A total of 82 histologic ROIs were evaluated:  $n_F = 26$ ,  $n_L = 13$ ,  $n_H = 10$ ,  $n_{FL} = 10$ ,  $n_{FH} = 2$ ,  $n_{LH} = 6$ ,  $n_{FCa} = 5$  and  $n_{Com} = 10$ . Of the 10 complex plaques, 9 were F-L-H plaques, and one was F-L-H-Ca.

### ULTRASONIC DATA ANALYSIS

We considered several analysis techniques of the RF and grey-scale measurements. The apparent backscatter transfer function (ABSTF) of a carotid plaque ROI was determined by spectral analysis of ultrasonic RF measurements using a sliding window technique, from which several parameters were determined. Images were then constructed from these parameters, and average parameter values are determined from ROIs selected from the quantitative parametric image. An alternative spectral technique analyzes an entire "block" of RF signals in contrast to the sliding window technique. For the present case, the blocks were identified based on point and line number coordinates of the ROIs previously selected from the parametric images. For each block, a single spatially averaged parameter value was obtained. A third approach is based upon the analysis of the grey-scale images.

#### Parametric image construction

RF analysis was performed in MATLAB (Version 6, The MathWorks, Inc., Natick, MA) using a sliding window (32-point Hamming gate corresponding to  $\sim 1$  mm) that was shifted along each RF line by 1 point between sequential windows (97% overlap). For each windowed segment of RF signal, the power spectrum was calculated from the magnitude squared of the fast Fourier transform for both the plaque ( $|F_{tissue}(\omega)|^2$ ) and the reference phantom ( $|F_{ref}(\omega)|^2$ ). The ABSTF is given by the ratio of the tissue power spectrum to the reference phantom power spectrum. We then considered several parameters based on a straight-line fit to the ABSTF (Lizzi et al. 1986), including the midband, slope and intercept values as graphically represented in Fig. 4. We also considered the IBS parameter, which is determined using the conventional expression (Bridal et al. 1997b):

$$IBS = \frac{1}{\omega_H - \omega_L} \int_{\omega_L}^{\omega_H} 10 \log_{10} \left( \frac{|F_{tissue}(\omega)|^2}{|F_{ref}(\omega)|^2} \right) d\omega, \quad (1)$$

where  $\omega_L$  and  $\omega_H$  are the lower and upper frequency bandwidth limits, respectively. Each resulting parameter estimate was mapped to a pixel of the quantitative parametric images. We note that neighboring pixels along the

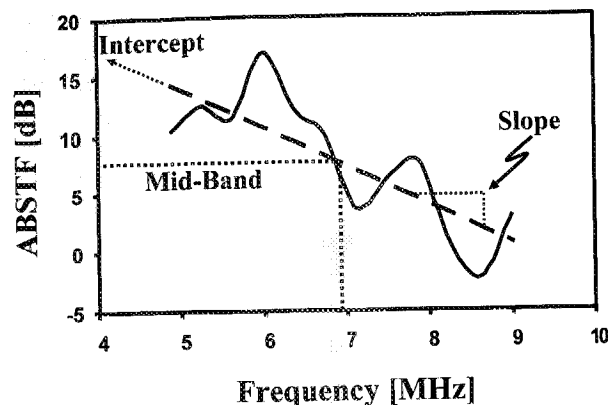


Fig. 4. Representative example of the apparent backscatter transfer function (ABSTF) over the frequency range 5 to 9 MHz (solid curve) determined by the ratio of the backscattered power from a region of carotid plaque to the backscattered power from a region of the tissue-mimicking phantom. Examples of parameters derived from the straight-line fit (---) to the ABSTF are also noted: midband, slope and intercept values.

depth axis of the quantitative image are not independent because of the high degree of window overlap.

#### Region-of-interest selection

Region-of-interest analysis was performed following the construction of the parametric images. The selection of the ROIs in the images of the plaque sections was limited to regions nearest to the face of the ultrasonic probe, to minimize effects due to path length attenuation in the tissue. Each individual ROI had dimensions of 1 mm  $\times$  1 mm (or, 32 points by 11 lines), and were independent (*i.e.*, no overlap with other ROIs). Efforts were made to avoid highly echogenic regions, which are typically associated with large calcifications, as previously mentioned. The ROIs were selected through the aid of a graphic interface of an in-house analysis software package. The same ROIs for a given plaque section were used for each parametric image. Each parameter was then spatially averaged within each ROI of the parametric image. A total of 82 ROIs were selected for ultrasonic analysis.

#### Block RF parametric analysis

A Hamming window of 64 points was applied to each RF line of the same ROI as that analyzed by the sliding window technique described above. (Note: Each pixel in a parametric image is the result of the analysis of 32 RF points. Consequently, a 32-point line in a parametric image determined using a sliding window, 32 point length, 1 point shift, corresponds to the analysis of 64 RF points.) The average power spectrum was then

calculated from the 11 lines of the ROI. The average power spectrum was calculated for matched regions of both the carotid plaque specimens and the reference phantom from which the ABSTF was calculated. The same parameters were calculated for the block-RF approach as were calculated for the sliding window approach.

#### Grey-scale analysis

Analysis of the grey-scale images was performed using the HDILab toolkit (Philips Ultrasound research signal and image processing software; Bothell, WA), where an attempt to remove the logarithmic compression and thresholding applied to the ultrasonic grey-scale signals has been performed. (These signals are sometimes referred to as grey-scale acoustic intensity, as discussed in the HDILab documentation.) ROIs of size 1 mm × 1 mm were selected in the grey-scale images corresponding to the ROIs of the parametric images. The procedure for transferring ROIs from parametric images to grey-scale images was the same as that for the ROIs of the histology images (*i.e.*, morphologic markers). The spatial average of the grey-scale value for each ROI was determined in the linear domain. We normalize the average grey-scale value of a ROI of a carotid plaque image by a corresponding average grey-scale value of a ROI of the phantom. Finally, the normalized grey-scale value is expressed in decibels.

#### Statistical analysis

To determine if we can differentiate the populations of different plaque types based on US parameter values, we used a nonparametric Kruskal-Wallis (K-W) comparison Z-value test (NCSS 2000, NCSS, Kaysville, Utah), which makes no assumptions regarding the distribution of parameter values (*e.g.*, normal). The null hypothesis is that there is no difference in the mean parameter values of the plaque types. The alternative hypothesis is that there is a difference in the mean parameter values of the plaque types. We choose a level of significance of 0.05.

Mean and standard deviations (SDs) are reported for each parameter and plaque type. The K-W analysis tested if mean parameter values for the different plaque types satisfied the alternative hypothesis. Statistical analysis was performed on 75 of the original 82 ROIs for the (sliding window and block) IBS and grey-scale parameters. Fibrohemorrhage plaques ( $n_{FH} = 2$ ) could not be compared using the K-W test because of the small population count, for which at least five samples are necessary. In addition, fibrocalcification plaques could not be included for the statistical analysis based on the assumption of equal variances of parameter values as a function

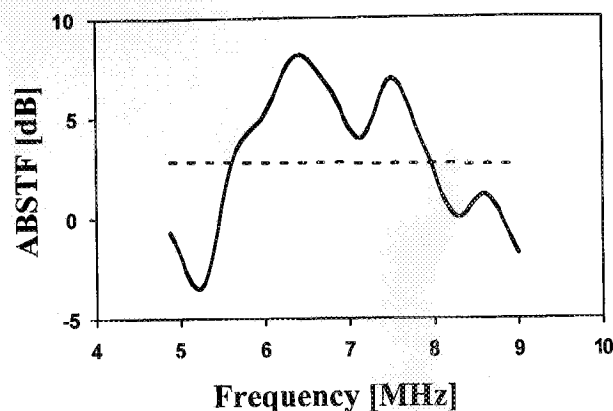


Fig. 5. Example of a straight-line fit to an ABSTF with a small correlation coefficient ( $r^2 < 0.001$ ). The ABSTF from a fibrolipid region over the frequency range 5 to 9 MHz is shown as the solid curve, and the fit to the ABSTF is given by the dashed line.

of plaque type (*i.e.*, the variance of the IBS parameters of the fibrocalcification population was too large).

Before calculating the means and SDs of the ultrasonic parameters based on the straight-line fit to the ABSTF (*i.e.*, midband, slope and intercept), we performed an additional statistical test (*t*-test,  $p < 0.05$ ) to determine if there was a significant correlation (Mould 1989) between the fit and ABSTF as determined by the block-RF analysis. This statistical test removed those fits with small correlation values (approx.  $r^2 < 0.32$ ) at the expense of reducing the population count of the plaques. Figure 5 provides an example of a poor straight-line fit to an apparent BS TF of a fibrolipid plaque that was removed from the population before statistical analysis. A total of 71% (58 ROIs) of the original 82 ROIs satisfied the *t*-test:  $n_F = 17$ ,  $n_L = 9$ ,  $n_H = 8$ ,  $n_{FL} = 8$ ,  $n_{FH} = 2$ ,  $n_{LH} = 6$ ,  $n_{FCa} = 3$  and  $n_{Com} = 5$ . The 5 remaining complex plaques contained collagen, lipid and hemorrhage. Fibrohemorrhage ( $n_{FH} = 2$ ) and fibrocalcification ( $n_{FCa} = 3$ ) plaques could not be compared using the K-W test because of the small population count. Further discussion of fitting the ABSTF with a straight line can be found in the Discussion section.

We also examined whether or not the different analysis techniques (*i.e.*, sliding window, block, and grey-scale) agree with one another. Based on a statistical analysis proposed by Bland and Altman (1986), the lack of agreement between two measurement methods is summarized by a bias and limits of agreement. The bias is estimated as the mean difference between the two measurements (*e.g.*, sliding window IBS and block IBS), and the limits of agreement (95% confidence level) are estimated as 2 times the SD of the differences.

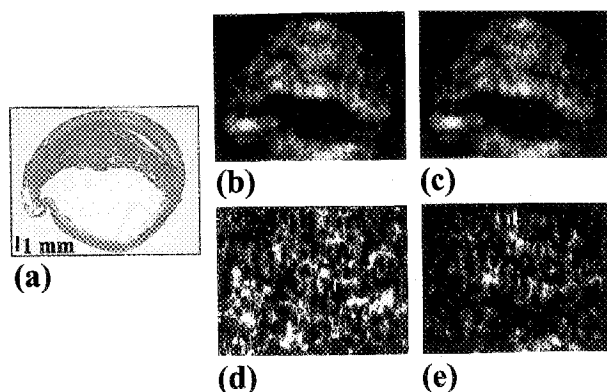


Fig. 6. Images (and corresponding grey-scale limits) of (a) histology, (b) IBS (-12 to 30 dB), (c) midband value (-12 to 30 dB), (d) slope (-4 to 4 dB/MHz), and (e) intercept (0 to 60 dB) of the straight-line fit to the apparent backscatter transfer function of a hemorrhage plaque. Each pixel represents an ultrasonic spectral parameter estimated from ~1 mm-long Hamming-gated segment of a RF line sampled using a digitizer connected to a Philips HDI 5000 imaging system. The plaque was stained with HES before capturing the histologic image with an optical magnifier.

## RESULTS

Representative images of histology and US parameters for a section of a hemorrhage plaque are shown in Fig. 6. Parametric images of the IBS (Fig. 6b) and midband value of the straight-line fit to the ABSTF (Fig. 6c) provided agreement in morphology with histology (Fig. 6a). Parametric images of the slope and intercept of the straight-line fit are shown in Fig. 6d, e, respectively. However, these images of local estimations of the slope and intercept parameters are very noisy due in part to the short sliding window used in the analysis (*i.e.*, 1-mm long Hamming-gated segments of RF lines using a 5- to 9-MHz bandwidth).

### Mid-band, slope and intercept parameters

The (sliding window and block) midband, slope and intercept parameter values as a function of plaque type are summarized in Fig. 7a, b, c. We include results for fibrocalcification and fibrohemorrhage plaques, but note that their small population counts preclude their use in the statistical analyses. These results include those 58 ROIs for which the line fits were significantly correlated with the (block) ABSTF, as discussed above. There was a bias of -0.7 dB between the sliding window and block midband parameters, with limits of agreement of 1.8 dB. Fibrous plaques were found to have a midband value near 6 dB. The midband value of the fibrous plaques was approximately 2 dB greater than lipid and lipid-hemorrhage plaques and 3 to 4 dB greater than hemorrhage and

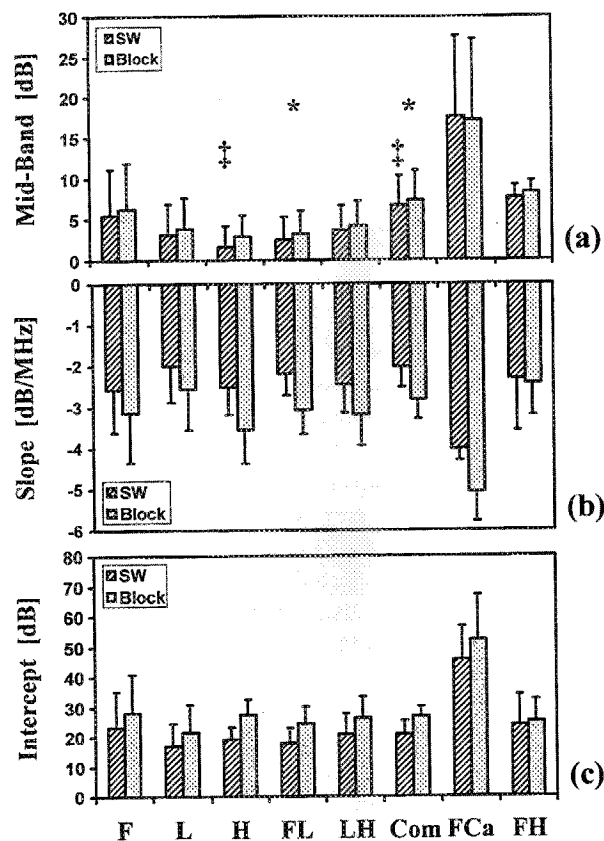


Fig. 7. Summary of (a) midband, (b) slope, and (c) intercept parameters (mean  $\pm$  SD) as a function of plaque type. Parameters were calculated using the sliding window (SW) and block-RF (block) techniques. \* mean midband values for complex and fibrolipid plaques were significantly different ( $p < 0.05$ ) for both the sliding window and block techniques. ‡ mean midband values for complex and hemorrhage plaques were significantly different ( $p < 0.05$ ) for only the sliding window technique.

fibrolipid plaques. Complex plaques (F-H-L) had a midband value 1 dB larger than fibrous plaques. A pairwise K-W statistical analysis indicated that the mean (sliding window and block) midband values were significantly different ( $p < 0.05$ ) for complex and fibrolipid plaques. The mean (block) midband values of the complex and hemorrhage plaques also satisfied the alternative hypothesis that the means were different.

The (sliding window and block) slope parameters of the plaque types are summarized in Fig. 7b. The lack of agreement between the sliding window and block slope parameters was  $0.7 \pm 1.1$  dB/MHz (bias  $\pm$  limits of agreement). The mean slope of the fibrous plaques was approximately -3 dB/MHz. The mean slope of the lipid plaques was 0.5 dB/MHz greater than that of the fibrous plaques. The mean slopes of the hemorrhage, fibrolipid

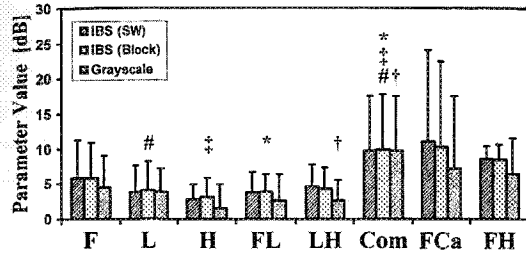


Fig. 8. Summary of sliding window (SW), integrated backscatter (IBS), block-RF IBS, and grey-scale parameters (mean  $\pm$  SD) as a function of plaque type. \* mean values for complex and fibrolipid plaques; ‡ mean values for complex and hemorrhage plaques; # mean values for complex and lipid plaques were significantly different for (sliding window and block) IBS and grey-scale parameters; and † mean values for complex and lipid-hemorrhage plaques were significantly different for only the GS parameter.

and lipid-hemorrhage plaques were within 0.5 dB/MHz of each other. A pairwise K-W statistical analysis found that the null hypothesis was satisfied based on the slope parameter of the plaque types, or that the mean slope values of the plaque types were the same ( $p < 0.05$ ).

The (sliding window and block) intercept parameters of the plaque types are shown in Fig. 7c. The lack of agreement between the sliding window and block intercept values was  $-5.6 \pm 7.7$  dB. The mean (block) intercept value of the fibrous plaques was largest (excluding the fibrocalcification plaques) at 28 dB. The mean intercept value of the lipid plaques was 6 dB smaller than that of the fibrous plaques. The mean intercept values of the remaining plaques fell between those of the fibrous and lipid plaques. Similar to the slope parameter, the null hypothesis ( $p < 0.05$ ) was satisfied for a pairwise K-W statistical analysis of the intercept parameters of the plaque types, in that the mean intercept values of the plaques were not significantly different.

#### Integrated backscatter and grey-scale parameters

Figure 8 summarizes the (sliding window and block) IBS and grey-scale parameters. In contrast to the parameter results based on the straight-line fit to the ABSTF, all 82 ROIs are reported in the IBS and grey-scale results. (We note that there is no reason *a priori* to exclude any ROIs, as was the case for parameters based on a straight-line fit to the apparent BS TF.) We again include the results for the fibrocalcification and fibrohemorrhage plaques, but do not attempt any statistical conclusions. The bias and limits of agreement between the sliding window and block IBS parameters was  $0.0 \pm 1.8$  dB (*i.e.*, no bias). The lack of agreement between the (sliding window or block) IBS and grey-scale parameters

was  $1.3 \pm 4.9$  dB. The mean IBS value of fibrous plaques were about + 6 dB relative to the phantom. The mean IBS values of lipid and hemorrhage plaques were 2 and 3 dB, respectively, below that of fibrous plaques. Similarly, fibrolipid and lipid-hemorrhage plaques both had mean IBS values 2 dB below that of fibrous plaques. The complex plaques had mean IBS values about 4 dB larger than that of the fibrous plaques. Relative differences between the grey-scale values of the plaque types were, in general, smaller than those of the corresponding IBS values. A pairwise K-W statistical analysis found a number of plaque pairs that satisfied the alternative hypothesis ( $p < 0.05$ ). All three parameters (*i.e.*, sliding window IBS, block IBS, and grey-scale) found the mean parameter value of the complex plaques to be different than that of the lipid, hemorrhage and fibrolipid plaques. In addition, the mean grey-scale parameter of the complex plaques was different from that of the lipid-hemorrhage plaques.

## DISCUSSION

This investigation used a clinical US imaging system with access to US RF signals and a tissue-mimicking phantom as a reference material in an effort to quantitatively evaluate carotid plaque content. Evaluation of plaque content was performed by ROI analysis of parametric images, block RF analysis of ultrasonic RF signals, and grey-scale analysis of clinical images. We have also considered a number of US parameters, including the IBS and several others based on a straight-line fit of the ABSTF.

#### Previous investigations

Previous measurements of atherosclerotic plaques have been performed under a variety of experimental conditions. Several *in vitro* and *ex vivo* investigations (Barzilai *et al.* 1987; Bridal *et al.* 2000, 1997a, 1997b; Nair *et al.* 2002; Noritomi *et al.* 1997b) have considered parameters based on the backscattering and attenuation properties as a function of plaque composition. These same investigations were performed with single-element transducers, and a planar reflector often used as a reference measurement. In contrast, another study (Takiuchi *et al.* 2000) used a linear-array transducer and a selected tissue type as a reference measurement. A preliminary *in vivo* investigation (Noritomi *et al.* 1997a) used a multiparametric approach to successfully distinguish between plaques with and without thrombus. This particular study used a 10-MHz mechanical sector-scanning transducer with an effective bandwidth of 3 to 13 MHz, and considered the slope and intercept of the straight-line fit to the ABSTF.

### *Ultrasonic parameters and histology*

The ultrasonic images of the IBS, midband and grey-scale parameters corresponded well with morphology of the histology images. In contrast, the ultrasonic images of the slope and intercept parameters were very noisy, and could not be said to agree with the morphology of the histology images. This parallels the observation that the IBS, midband and grey-scale parameters were able to distinguish plaque types based on the pairwise K-W test of mean parameter values, whereas the slope and intercept parameters could not distinguish plaque types. In particular, the complex plaque type was common to each plaque pair found to have different mean parameter values (*i.e.*, Complex-L, Complex-H, Complex-FL and Complex-LH).

The mean IBS value for fibrous plaques was approximately 2 dB larger than that of lipid plaques. Because of the role played by collagen and lipid in plaque stability, this difference of 2 dB is of particular interest. However, we remark that the difference between mean values of the fibrous and lipid plaques was not found to be statistically meaningful. This could be due in part to the large variances and small population counts. Other researchers (Barzilai et al. 1987) found a difference of 3.2 dB in IBS (bandwidth: 3 to 13 MHz) between fibrous and fibrolipidic plaques, whereas the current results show a difference near 2 dB. In addition, the approximately 1-dB difference in average IBS values measured between lipid and hemorrhage plaques is consistent with the observation that it is difficult to separate these two types of plaque using the IBS parameter alone (Bridal et al. 2000). Noritomi et al. (1997a) found significant differences (*t*-test,  $p < 0.01$ ) of  $-0.48$  dB/MHz and  $+5.6$  dB between the mean slopes and intercepts, respectively, of fibrous and lipid plaques. These differences compare well with the present measurements ( $-0.59$  dB/MHz and  $+6.4$  dB), although statistical significance was, again, not found. We note that Noritomi and colleagues measured statistical significance using a parametric *t*-test, whereas we have employed the nonparametric K-W test. It is known that parametric tests are more sensitive than nonparametric tests, but come at the cost of restricting the distribution of values (*e.g.*, parameter values are normally distributed).

### *Sources of variance*

The sources of variance in US spectral parameters have been well described for parameter image construction (Lizzi et al. 1997) and ROI spectral averaging (Huisman and Thijssen 1996), as in the case of the block-RF analysis. Considering experimental factors, such as the bandwidth and the short RF windows along with the effects of stochastic tissue microstructure in a homogeneous tissue, one could expect the SDs of the parameters

determined by the sliding window technique to be on the order of 3 to 4 times larger than those determined by the block-RF technique. As a means to reduce the SD of spectral estimates, a number of alternative strategies have been suggested that include using a larger bandwidth (Lizzi et al. 1997), smoothing of local estimates in spectrally homogeneous regions (Gorce et al. 2002), increasing the number of RF lines used for the estimation of the average spectrum from the reference scattering medium (Huisman and Thijssen 1996) and using spectral estimators that may be more accurate than the classic Fourier methods (Nair et al. 2001). In addition to the variance due to spectral estimation techniques, heterogeneity in tissues will further increase the SD of the parameter estimates.

### *Bias and limits of agreement*

Measuring agreement between parameters and analysis techniques was assessed by a bias with limits of agreement. This included comparison of like parameters determined by the sliding window and block techniques (*i.e.*, IBS, midband, slope and intercept). In addition, we compared the (sliding window and block) IBS parameters with the grey-scale parameter. It is also possible to compare different parameters based on the same analysis technique that provide an estimate of the same quantity. For example, the IBS and midband parameters both provide an estimate of an average backscattered power.

We found various levels of agreement when comparing the same parameters calculated by the sliding window and block techniques. The IBS and midband parameters exhibited better agreement, with the IBS parameter appearing to be most robust ( $0.0 \pm 1.7$  dB) between analysis techniques. The bias between the sliding window and block midband parameters was  $-0.7$  dB, and had limits of agreement of  $\pm 1.9$  dB. Agreement was  $0.7 \pm 1.1$  dB/MHz and  $-5.6 \pm 7.7$  dB for the slope and intercept parameters, respectively. If we, instead, compared different parameters for a given analysis technique (*i.e.*, sliding window or block), we found the agreement between the sliding window IBS and sliding window midband was  $0.8 \pm 0.7$  dB. The agreement between block IBS and block midband was  $0.2 \pm 0.4$  dB. The grey-scale parameter provided still another alternative estimate of an average backscattered power. Comparison of the grey-scale and (sliding window or block) IBS parameter found a bias with limits of agreement of  $1.3 \pm 4.9$  dB.

The question of whether or not parameters or techniques are interchangeable depends in part upon the size of differences that can be tolerated. For example, one may find that the IBS and midband parameters can be used interchangeably, given the relatively small biases and tight limits of agreement. On the other hand, it is

unlikely that the IBS and grey-scale parameters could be used interchangeably considering the bias and relatively large limits of agreement. This discrepancy exists in part due to the normalization of the grey-scale value of a plaque region by the grey-scale value of a TM phantom not being strictly a substitution technique. This analysis of bias and limits of agreement indicates that one must use caution when comparing absolute results between studies.

#### *Significant correlation of straight-line fits*

Previous studies (Bridal *et al.* 2000; Lizzi *et al.* 1983; Nair *et al.* 2002; Noritomi *et al.* 1997b) have demonstrated the usefulness of considering several parameters for the evaluation of plaque content. In particular, parameters derived from a straight-line fit (*e.g.*, slope and intercept) to the ABSTF have often been considered. The original analytical framework developed by Lizzi *et al.* (1986) for fitting the ABSTF with a straight line is based on a number of assumptions, including in part, that any given ROI be considered homogeneous with a uniform size distribution of scatterers. However, as we have observed for some of the atherosclerotic plaque specimens of this investigation, the ABSTF could not be reasonably fit by a straight line (see Fig. 5), nor can we be certain that all ROIs are homogeneous over length scales ( $\sim 1$  mm) considered here. This in turn questions the efficacy of using parameters based on a straight-line fit that may not be appropriate. Consequently, we performed a statistical *t*-test ( $p < 0.05$ ) to exclude those plaque ROIs with ABSTFs that could not be fit reasonably with a straight line. This excluded approximately 30% of the original 82 ROIs.

It is instructive to consider how the mean slope and intercept parameter values would change if we did not test for significant correlation. The mean slope values for fibrous, lipid, and hemorrhage plaques would increase on average by approximately 0.5 dB/MHz. The corresponding mean intercept values decrease on average by 2 to 5 dB. Perhaps most notable, however, is that the mean sliding window slope values for lipid-hemorrhage and complex plaques would be statistically different. In addition, lipid and lipid-hemorrhage plaques would have statistically different mean (Block) slope values. This analysis illustrates the concern one has regarding the appropriateness of a straight-line fit to the ABSTF. In many cases, the ABSTF may not be reasonably modeled as being proportional to frequency. If one were to 'blindly' apply the straight-line fit to all the plaque ROIs, we would conclude that some plaque pairs could be differentiated by the slope parameter. Assuming that the analysis of the reduced set of ROIs (*t*-test selected) is more accurate, we would then have a false positive. In

other words, the null hypothesis would be incorrectly rejected.

The present investigation serves as a step toward the use of ultrasound for the quantitative evaluation of carotid plaque under *in vivo* conditions. There are, however, several limitations of the present study that must be addressed in future investigations. First, fixation is known to affect the ultrasonic properties of tissue. Some research suggests that changes to the qualitative ultrasonic backscattering properties of plaque due to fixation are not significant (Hiro *et al.* 2001). However, formalin-fixative solutions have been shown to increase cross linking in collagenous tissues (Hall *et al.* 2000), with an accompanying increase in the magnitude and slope of attenuation. This increase in attenuation would, in principle, lead to a decrease in the level of backscattered US from collagenous regions and perhaps a reduction in the difference in levels of backscatter between collagen and other plaque types. Further study regarding the effects of fixation on various plaque types is consequently of potential interest. Alternative experimental protocols, including ultrasound measurements before fixation (*i.e.*, on 'fresh' tissue) or following the freezing of tissue (Bridal *et al.* 1997b), can avoid issues related to the fixation of tissue. Second, plaque sections selected for measurement in this current study were based on the criterion of maximum stenosis, which, in part, limited the number of measurements. Obtaining larger populations of plaque types could be achieved by imaging at periodic positions along the plaque length (*e.g.*, every 1 mm) as has been performed in other investigations (Noritomi *et al.* 1997b). Last, a better understanding of how plaque composition affects the propagation and scattering properties of the US can lead to determination of what are the most appropriate parameters for the differentiation of plaque type for given experimental conditions. It remains a related topic of continuing research as to the observation that average-like parameters (*e.g.*, IBS) provide better morphologic agreement to histology than do derivative-like parameters (*e.g.*, slope).

#### SUMMARY

We have performed *in vitro* measurements of fixed, human carotid plaque specimens using a 7.5-MHz linear array of a clinical US imaging system capable of acquiring both grey-scale images and ultrasonic RF signals. A tissue-mimicking phantom served as a reference material. We considered the IBS and the midband, slope and intercept values derived from a straight-line fit to the ABSTF. For certain plaque ROIs, the straight-line fits and ABSTF were not significantly correlated and, consequently, those ROIs were removed from the population before any statistical analysis. The IBS and midband

parameters provided good agreement in morphology with the histology images. In addition, parameters based on an average backscattered power (*i.e.*, IBS, midband and grey-scale) were found to be more sensitive to plaque type than those parameters based on the frequency dependence of the backscattered power (*i.e.*, slope and intercept). Complex plaques had significantly different mean IBS, midband and grey-scale parameter values compared to those parameter values of lipid, hemorrhage and fibrolipid plaques. The IBS and midband parameters appeared to be interchangeable for the characterization of carotid plaque content, based on a statistical analysis of the bias and limits of agreement. However, the grey-scale technique did not appear to be interchangeable with either the sliding window or block-RF techniques. The present investigation identifies several improvements in experimental techniques to benefit future studies, and serves as a step toward the quantitative evaluation of carotid plaques under *in vivo* conditions.

## REFERENCES

- Barzilai B, Saffitz J, Miller JG, Sobel B. Quantitative ultrasonic characterization of the nature of atherosclerotic plaques in human aorta. *Circ Res* 1987;60:459-463.
- Bland JM, Altman DG. Statistical methods for assessing agreement between two methods of clinical measurement. *Lancet* 1986;1:307-310.
- Bridal SL, Beyssen B, Fornès P, Julia P, Berger G. Multiparametric attenuation and backscatter images for characterization of carotid plaque. *Ultrasound Imaging* 2000;22:20-34.
- Bridal SL, Fornès P, Bruneval P, Berger G. Correlation of ultrasonic attenuation (30 to 50 MHz) and constituents of atherosclerotic plaque. *Ultrasound Med Biol* 1997a;23:691-703.
- Bridal SL, Fornès P, Bruneval P, Berger G. Parametric (integrated backscatter and attenuation) images constructed using backscattered radiofrequency signals (25-56 MHz) from human aortae *in vitro*. *Ultrasound Med Biol* 1997b;23:215-229.
- Campbell JA, Waag RC. Normalization of ultrasonic scattering measurements to obtain average differential scattering cross sections for tissues. *J Acoust Soc Am* 1983;74:393-399.
- Coy KM, Park JC, Fishbein MC, et al. In vitro validation of three-dimensional intravascular ultrasound for the evaluation of arterial injury after balloon angioplasty. *J Am Coll Cardiol* 1992;20:692-700.
- Davies M, Thomas A. Plaque fissuring—The cause of acute myocardial infarction, sudden ischaemic death, and crescendo angina. *Heart* 1985;53:363-373.
- de Korte CL, van der Steen AFW, Cespedes EI, et al. Characterization of plaque components and vulnerability with intravascular ultrasound elastography. *Phys Med Biol* 2000;45:1465-1475.
- Fink MA, Cardoso J-F. Diffraction effects in pulse-echo measurement. *IEEE Trans Sonics Ultrason* 1984;31:313-329.
- Gorce J-M, Friboulet D, Dydenko I, et al. Processing radio frequency ultrasound images: A robust method for local spectral features estimation by a spatially constrained parametric approach. *IEEE Trans Ultrason Ferroelec Freq Control* 2002;49:1704-1719.
- Gronholdt ML, Nordestgaard B, Wiebe BM, Wilhjelmsen J, Sillesen H. Echo-lucency of computerized ultrasound images of carotid atherosclerotic plaques are associated with increased levels of triglyceride-rich lipoproteins as well as increased plaque lipid content. *Circulation* 1998;97:34-40.
- Gronholdt ML, Wiebe BM, Laursen H, et al. Lipid-rich carotid artery plaques appear echolucent on ultrasound B-mode images and may be associated with intraplaque haemorrhage. *Eur J Vasc Endovasc Surg* 1997;14:439-445.
- Hall CS, Dent CL, Scott MJ, Wickline SA. High-frequency ultrasound detection of the temporal evolution of protein cross linking in myocardial tissue. *IEEE Trans Ultrason Ferroelec Freq Control* 2000;47:1051-1058.
- Hiro T, Fujii T, Yasumoto K, et al. Detection of fibrous cap in atherosclerotic plaque by intravascular ultrasound by use of color mapping of angle-dependent echo-intensity variation. *Circulation* 2001;103:1206-1211.
- Huisman HJ, Thijssen JM. Precision and accuracy of acoustospectrographic parameters. *Ultrasound Med Biol* 1996;22:855-871.
- Lizzi FL, Astor M, Feleppa EJ, Shao M, Kalisz A. Statistical framework for ultrasonic spectral parameter imaging. *Ultrasound Med Biol* 1997;23:1371-1382.
- Lizzi FL, Greenebaum M, Feleppa EJ, Elbaum M, Coleman DJ. Theoretical framework for spectrum analysis in ultrasonic tissue characterization. *J Acoust Soc Am* 1983;73:1366-1373.
- Lizzi FL, Ostromogilsky M, Feleppa EJ, Rorke MC, Yaremko MM. Relationship of ultrasonic spectral parameters to features of tissue microstructure. *IEEE Trans Ultrason Ferroelec Freq Control* 1986;33:319-329.
- Loree HM, Kamm RD, Stringfellow RG, Lee RT. Effects of fibrous cap thickness on peak circumferential stress in model atherosclerotic vessels. *Circ Res* 1992;71:850-858.
- Lusis AJ. Atherosclerosis. *Nature* 2000;407:233-241.
- Madsen EL. Method of determination of acoustic backscatter and attenuation coefficients independent of depth and instrumentation. In: Shung KK, Thieme GA, eds. *Ultrasonic scattering in biological tissues*. Boca Raton, FL: CRC Press, 1993:205-250.
- Mould RF. *Introductory medical statistics*. Bristol: Institute of Physics, 1989.
- Nair A, Kuban BD, Obuchowski N, Vince DG. Assessing spectral algorithms to predict atherosclerotic plaque composition with normalized and raw intravascular ultrasound data. *Ultrasound Med Biol* 2001;27:1319-1331.
- Nair A, Kuban BD, Tuzcu EM, et al. Coronary plaque classification with intravascular ultrasound radiofrequency data analysis. *Circulation* 2002;106:2200-2206.
- NASCET (North American Symptomatic Carotid Endarterectomy Trial collaborators). Beneficial effect of carotid endarterectomy patients with high grade carotid stenosis. *N Engl J Med* 1991;325:445-453.
- Noritomi T, Sigel B, Gahtan V, et al. In vivo detection of carotid plaque thrombus by ultrasonic tissue characterization. *J Ultrasound Med* 1997a;16:107-111.
- Noritomi T, Sigel B, Swami V, et al. Carotid plaque typing by multiple-parameter ultrasonic tissue characterization. *Ultrasound Med Biol* 1997b;23:643-650.
- Picano E, Landini L, Lattanzi F, et al. Ultrasonic tissue characterization of atherosclerosis: State of the art 1988. *J Nucl Med Allied Sci* 1988;32:174-185.
- Takiuchi S, Rakugi H, Honda K, et al. Quantitative ultrasonic tissue characterization can identify high risk atherosclerotic alteration in human carotid arteries. *Circulation* 2000;102:766-770.
- Urbani MP, Picano E, Parenti G, et al. In vivo radiofrequency-based ultrasonic tissue characterization of the atherosclerotic plaque. *Stroke* 1993;24:1507-1512.
- Wilhjelmsen J, Gronholdt M, Wiebe B, et al. Quantitative analysis of ultrasound B-mode images of carotid atherosclerotic plaque: Correlation with visual classification and histological examination. *IEEE Trans Med Imag* 1998;17:910-922.
- Zagzebski JA, Yao LX, Boote EJ, Lu ZF. Quantitative backscatter imaging. In: Shung KK, Thieme GA, eds. *Ultrasonic scattering in biological tissues*. Boca Raton, FL: CRC Press, 1993:451-486.